Perpendicular magnetic anisotropy and spin reorientation transition in L10 FePt films

Jae Young Ahn, Nyun Jong Lee, Tae Hee Kim, J.-H. Lee, Anny Michel, and Dominique Eyidi

Citation: Journal of Applied Physics **109**, 07B760 (2011); doi: 10.1063/1.3562506
View online: http://dx.doi.org/10.1063/1.3562506
View Table of Contents: http://scitation.aip.org/content/aip/journal/jap/109/7?ver=pdfcov
Published by the AIP Publishing

Perpendicular magnetic anisotropy and spin reorientation transition in $L1_0$ FePt films

Jae Young Ahn,[1] Nyun Jong Lee,[1] Tae Hee Kim,[1,a)] J.-H. Lee,[2] Anny Michel,[3] and Dominique Eyidi[3]
[1]*Department of Physics, Ewha Womans University, Seoul 120-750, South Korea*
[2]*Partron Co., LTD., Hwaseong-si, Gyeonggi-do 445-170, South Korea*
[3]*Département de Physique et Mécanique des Matériaux, Institut Pprime, UPR 3346, CNRS-Université de Poitiers-ENSMA, SP2MI–Téléport 2, F86962 Futuroscope-Chasseneuil cedex, France*

(Presented 16 November 2010; received 5 October 2010; accepted 2 December 2010; published online 8 April 2011)

We investigated the thickness and composition dependence of perpendicular magnetic anisotropy (PMA) in $L1_0$ $Fe_{1-x}Pt_x$ ($x=0.4$, 0.5, and 0.55) films. The FePt films with different thicknesses of 35 and 70 Å were grown at the substrate temperature $T_s=300$ °C by molecular beam epitaxy coevaporation technique. A (001)-oriented epitaxial $L1_0$ FePt film was grown on the thin (001)-oriented fcc Pt layer, while a poorly crystallized FePt film was formed on the (111)-textured Pt layer. Our results showed that, at a fixed thickness of 70 Å, the PMA of FePt alloy films is enhanced as Pt content increases from 40% to 55%. © *2011 American Institute of Physics*. [doi:10.1063/1.3562506]

Since the large uniaxial magnetocrystalline anisotopy of $L1_0$-ordered FePt alloys allows the perpendicular magnetization in the thin film geometry, these alloys have been extensively studied for applications of the terabit-range high-density magnetic recording media.[1,2] However, a high T process required to form the $L1_0$-ordered structure is a disadvantage for practical application because high temperature durable materials for hard disk drives have yet to be discovered. In order to improve upon the high T process, i.e., deposition on a heated substrate and postannealing above 500 °C, several endeavors on the low T deposition of FePt were made. Rapid thermal annealing of disordered FePt films deposited directly on glass at room temperature (RT) was investigated,[3] but a strong in-plane contribution was reported. Influences of the buffer layers[4,5] and off-stoichiometry[6] on the PMA in FePt films sputter deposited at reduced temperatures also have been explored as alternatives. For the Pt-rich compounds, the PMA was obtained even in the case of the $T_s=300$ °C, which is rather irrelevant to the buffer layers, such as Au, Pt, and PtAu, whereas the $L1_0$ phase with PMA in the Fe-rich compounds has been observed only for the film with an Au buffer layer.

Our aim was to study the optimum growth condition and composition for low-T fabrication of highly ordered $L1_0$-FePt (001) films. We investigated the relation between the appearance of PMA and the $L1_0$ (001) texture of the FePt thin films as a function of film thickness and Pt compositions.

Thin films of $Fe_{1-x}Pt_x$ ($x=0.4$, 0.5, and 0.55) were grown by coevaporation of Fe and Pt under UHV conditions. During the deposition, the film composition and uniformity were controlled to better than ±1.0% by two independent quartz crystal rate monitors located inside the MBE chamber and by keeping the low deposition rate, ~0.03–0.05 Å/s. Fe–Pt films of 35–70 Å thickness were deposited at $T_s=250$ and 300 °C beyond the epitaxial Pt/MgO(001) buffer layer grown on chemically etched Si(100) substrates. During the deposition the pressure was kept below 5×10^{-9} Torr. T_s of the 50- to 100-Å-thick MgO was optimized at 200 °C. An Fe seed layer of 10 Å and subsequently a Pt buffer layer of 100 (or 50) Å were deposited at 70 °C. After codeposition of Fe and Pt, the samples were followed by *in situ* annealing at 300 °C for 1 h. Then, 30-Å-thick Al_2O_3 film was deposited as a capping layer. The detailed descriptions of samples are given in Table I.

Structural characterizations of the films were performed by XRD with Cu-$K\alpha$ radiation and a graphite monochromator. TEM specimen from selected FePt samples was prepared in cross section. A JEOL 2200FS microscope operating at 200 kV was used to observe the crystal structure of these films. The magnetic properties were measured at RT by a vibrating sample magnetometer.

Figure 1 corresponds to a representative texture analysis using dark field imaging for the $Fe_{0.5}Pt_{0.5}$ films grown at 250 °C. The bright field image in Fig. 1(a) shows, from bottom to top, the Si substrate, the 5-nm-thick MgO buffer layer (note that this layer is well crystallized but some layer roughness is observable), and the metallic epilayer. The small differences in lattice parameter and absorption coefficient do not allow a clear distinction between the 10 nm Pt layer and the 5 nm of FePt that were deposited on top. Dark field images were obtained by using the diffraction spots indicated in the selected area diffraction pattern in the inset of Fig. 1(a). The MgO layer [Fig. 1(b)], although consisting of several lateral grains, always adopts the [002] growth direction. On the other hand, the metallic layers show strong (002) texture [Fig. 1(d)] associated with a wide lateral grain size, but separated by narrow columnar grains with a (111) orientation, which are slightly inclined to the growth direction. One of the main results that should be underlined here is that the microstructure of the FePt deposited layer follows exactly the one of the Pt buffer layer, which, in turn, makes it impossible to distinguish those two layers; that means that, for the

a)Electronic mail: taehee@ewha.ac.kr.

TABLE I. Sample description.

	Substrate and layers
1	Si(100)\80 Å MgO\100 Å Pt\70 Å $Fe_{0.5}Pt_{0.5}$\30 Å Al_2O_3
2	Si(100)\80 Å MgO\10 Å Fe \100 Å Pt\70 Å $Fe_{0.5}Pt_{0.5}$\30 Å Al_2O_3
3	Si(100)\80 Å MgO\10 Å Fe \50 Å Pt\70 Å $Fe_{0.5}Pt_{0.5}$\30 Å Al_2O_3
4	Si(100)\80 Å MgO\10 Å Fe \50 Å Pt\35 Å $Fe_{0.5}Pt_{0.5}$\30 Å Al_2O_3
5	Si(100)\50 Å MgO\10 Å Fe \100 Å Pt\55 Å $Fe_{0.5}Pt_{0.5}$\30 Å Al_2O_3
6	Si(100)\80 Å MgO\10 Å Fe \50 Å Pt\70 Å $Fe_{0.6}Pt_{0.4}$\30 Å Al_2O_3
7	Si(100)\80 Å MgO\10 Å Fe \50 Å Pt\70 Å $Fe_{0.45}Pt_{0.55}$\30 Å Al_2O_3

epitaxial growth, the important interface is actually Pt-on-MgO, and that interface is the one guiding the orientation distribution in the Pt layer. These TEM observations prompted us to improve further the microstructure at the interfaces between MgO/Pt and Pt/FePt by increasing T_s from 250 to 300 °C during the growth of the FePt films.

XRD patterns for the $Fe_{0.5}Pt_{0.5}$ films grown on a Pt/MgO(001) buffer are shown in Fig. 2(a) as follows: (1) film grown without a Fe seed layer, (2) film grown on the 100-Å-thick Pt with a Fe seed layer, and (3) film grown under the same conditions as case 2, except for the Pt thickness being reduced to 50 Å. The pattern from sample 1 shows that without a Fe seed layer, a poorly crystallized FePt film is formed on (111)-textured Pt layer. On the other hand, when initiating the growth with a Fe seed layer, the Pt buffer is strongly (001) textured, and consequently the FePt films are also predominantly (001) textured. Mainly the (002) FePt diffraction peak is observed, but a weak contribution from (200) oriented grains can also be detected, as shown in Fig. 2(b). The FePt (001) superlattice peak, associated with the $L1_0$-ordered structure, is mostly visible in Fig. 2(a) for sample 3; and the superlattice peak position appears quite close to the position expected from the reference data. This good agreement supports the fact that the FePt phase deposited under these conditions is stoichiometric.

The order parameter[7] s was calculated as the ratio of the total intensities of the superlattice (001) to the fundamental (002) FePt peaks. As can be seen in Fig. 2(b), a fitting of the overlapping Pt (002), FePt (200), and FePt (002) peaks was necessary in order to obtain the relevant FePt (002) integrated intensity. In the case of sample 3, the calculation gives a value $s = 0.6 \pm 0.15$, the relatively large error being linked to the above-mentioned fitting procedure. Calculated values for other samples with a thin Pt buffer layer would actually point to a higher value of s. However, for the whole series of samples, the intrinsic peak broadening due to the very small thickness of the FePt layer, associated with an unfavorable thickness ratio to the Pt buffer layer, leads to an overlapping of the buffer and the FePt film signals, thus preventing a very accurate quantification Thus, the XRD-based determination of the s unreliable.

As for the slightly low value of $s = 0.6 \pm 0.15$, this result can be simply related to the low temperature employed during film growth. As a matter of fact, the s is known to increase with higher T_s; therefore, in this study the choice of low T_s was put forward at the expense of the s.

Figure 3 shows the change in magnetic anisotropy (MA) as a function of the FePt thickness: the normalized magnetization (M) curves measured at RT for film thickness of 35 and 70 Å are shown in Figs. 3(a) and 3(b), respectively. The M–H loops in Fig. 3(b) correspond to sample 3. The easy M axis is in a direction perpendicular to the film plane for sample 3. This is quite consistent with the XRD patterns shown in Fig. 2, where the (001) superlattice peak is clearly observed in sample 3. However, for the 35-Å-thick films

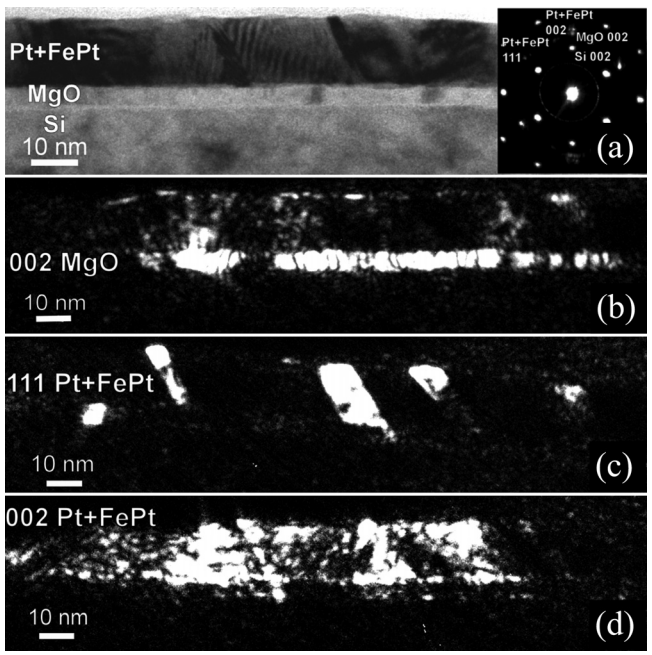

FIG. 1. Dark field imaging used for texture characterization: (a) Bright field image and corresponding selected area diffraction pattern in the inset, (b) 002-oriented MgO buffer layer, (c) small 111-oriented grains in the metallic (Pt + FePt) layer, and (d) wide grains with the preponderant 002 orientation in the Pt and FePt layers.

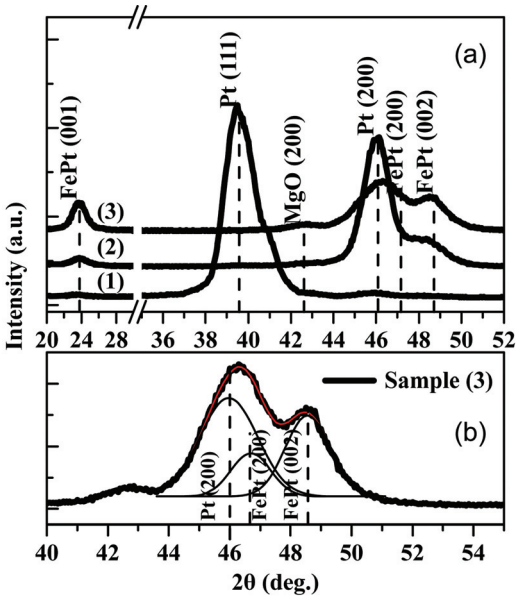

FIG. 2. (Color online) X-ray diffraction θ–2θ scans around (a) 20°–52° and (b) 42°–52° with Cu $K\alpha$ radiation for samples 1, 2, and 3: see Table I. In order to form the fct-FePt structure 10 nm MgO/1 nm Fe/5–10 nm Pt multilayer was deposited as a buffer; the dashed lines represent FePt peak positions from the powder diffraction file and solid lines represent the Gaussian fitting.

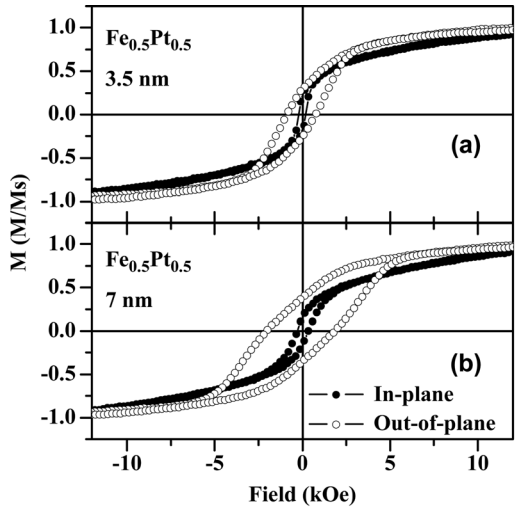

FIG. 3. Normalized magnetization curves measured at room temperature for (a) sample 4 and (b) sample 3. The magnetic field is applied in the perpendicular direction to the film (open circles, $H_{\perp}$) and in the in-plane direction (closed circles, $H_{//}$).

(sample 4) we observed an isotropic M in both $H_{\perp}$ and $H_{//}$ directions. These results show that the easy M axis perpendicular to the film plane could result from the formation of the $L1_0$-ordered structure with a strong [002] texture. However a low squareness ratio of M–H loop (M_r/M_s) is obtained; the ratios M_r/M_s with $H_{\perp}$ and $H_{//}$ are 0.4 and 0.2, respectively. This could be attributed to an incomplete formation of $L1_0$ phase ordering in the FePt film.

The normalized M curves measured at RT for different FePt composition are summarized in Fig. 4. For the $Fe_{0\cdot5}Pt_{0\cdot5}$ grown at 250 °C the M–H loops indicate the presence of non-negligible in-plane easy axis MA with predominant PMA. This is consistent with the TEM results (see Fig. 1), showing the existence of FePt (001) and (111) textures. The M–H loops for the $Fe_{1-x}Pt_x$ films grown at 300 °C and corresponding to $x = 0.4$ and 0.55 are shown in Figs. 4(b) and 4(c), respectively. The easy M axis perpendicular to the film plane occurs in samples 3, 5, 6, and 7 (see Table I), as shown in Fig. 3(b) and Fig. 4. It can be seen that perpendicular coercivity fields are roughly similar ($H_c = \sim 2$–3 kOe) for the samples, but the perpendicular M_r/M_s is considerably different. The ratios of the perpendicular to the in-plane remanence for samples 3, 5, 6, and 7 are 1.45, 1.17, 2.47, and 2.53, respectively. This is quite consistent with the strengthening of the [002] texture with increasing T_s found by the XRD. The relatively enhanced PMA that occurs with increasing Pt content is also worth mentioning.

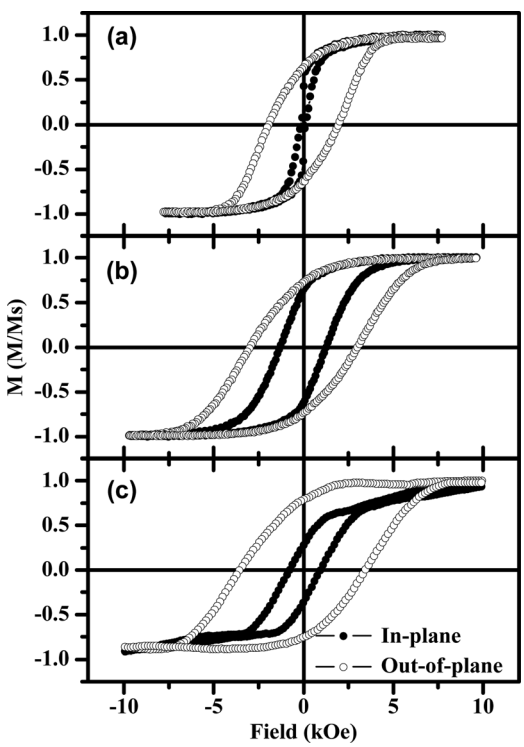

FIG. 4. Normalized magnetization curves measured at room temperature for (a) sample 5, (b) sample 6, and (c) sample 7. The magnetic field is applied in the perpendicular direction to the film (open circles) and in the in-plane direction (closed circles).

Since, for a fixed thickness of 70 Å, the lattice mismatch between Pt and FePt layers becomes smaller with increasing Pt content, a strain-free pseudomorphic growth could be possible. Moreover, the large spin-orbit coupling could be of importance in the Pt-rich compounds; therefore, the observed PMA could be attributed to the inversed SRT resulting from the change in magnetic energy at the interface between Pt/FePt with varying FePt composition as well as film thickness.

As is well known, nucleation of reverse domains is most likely at chemical or physical defects where the crystal anisotropy is lowered, thus the low values of H_c ($2-3$ kOe) in our FePt films could be related to the slightly low value of s (0.6 ± 0.15).[8–10] One might expect to observe an extremely high coercivity for highly ordered films. However, the earlier studies have also reported that the highest MA does not always correspond to the highest-s.[8]

In this work, we report the composition and thickness dependence of PMA in the epitaxial $Fe_{1-x}Pt_x$ thin films, parameters directly related to the film growth. The optimum growth conditions for low T process were investigated in order to achieve a high $L1_0$- ordered phase by using an appropriate buffer layer. However, additional work is planned in order to improve optimization and to enlighten the relation between PMA and spin reorientation transition in this system.

The authors gratefully acknowledge financial support by the Fundamental R&D Program for Core Technology of Materials funded by the Ministry of Knowledge Economy, South Korea and the National Research Foundation of Korea (NRF) through the Quantum Meta-Materials Research Center.

[1]S. Sun *et al.*, Science **287**, 1989 (2000).
[2]T. Klemmer *et al.*, Scr. Metall. Mater. **33**, 1793 (1995).
[3]Y. K. Takanashi *et al.*, Jpn. J. Appl. Phys. **40**, L1367 (2001).
[4]Y.-N. Hsu *et al.*, J. Appl. Phys. **89**, 7068 (2001).
[5]T. Seki *et al.*, Appl. Phys. Lett. **82**, 2461 (2003).
[6]T. Seki *et al.*, IEEE. Trans. Magn. **40**, 2522 (2004).
[7]A. Cebollada *et al.*, *Magnetic Structures*, edited by H. S. Nalwa (American Scientific, Los Angeles, 2002), pp. 93–122.
[8]K. Barmak *et al.*, J. Appl. Phys. **98**, 033904 (2005).
[9]K. M. Seeman *et al.*, Phys. Rev. B **76**, 174435 (2007).
[10]J. Y. Ahn, N. J. Lee, and T. H. Kim, J. Magn. **14**, 144 (2009).